

AMMA06
Field Program on the NOAA Ship Ronald H. Brown
May 27 – July 14, 2006

Results from the ETL Cloud and Flux Group and University of Miami Measurements

C. W. Fairall, Sergio Pezoa, Ludovic Bariteau, Ieng Jo
NOAA Environmental Technology Laboratory
Boulder, CO USA
June 15, 2006

1. Selected Samples for Julian Day 164

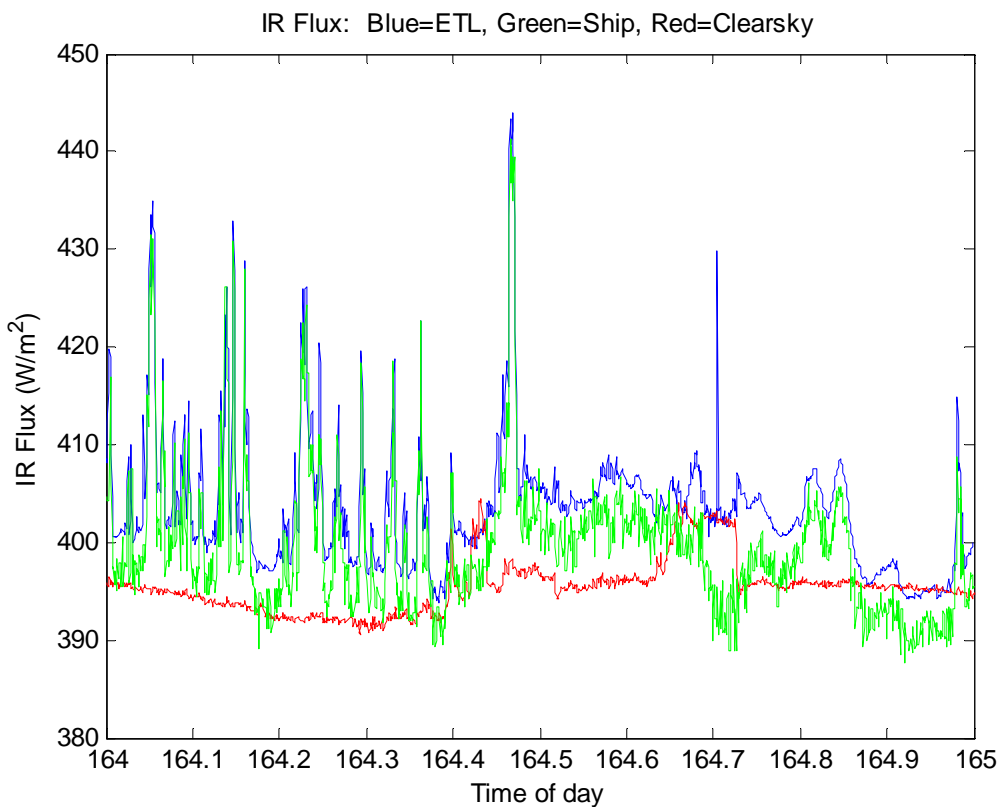


Figure 1. Time series of downward IR flux from ETL and ship Eppley sensors. The red line is a model of the expected clear sky value.

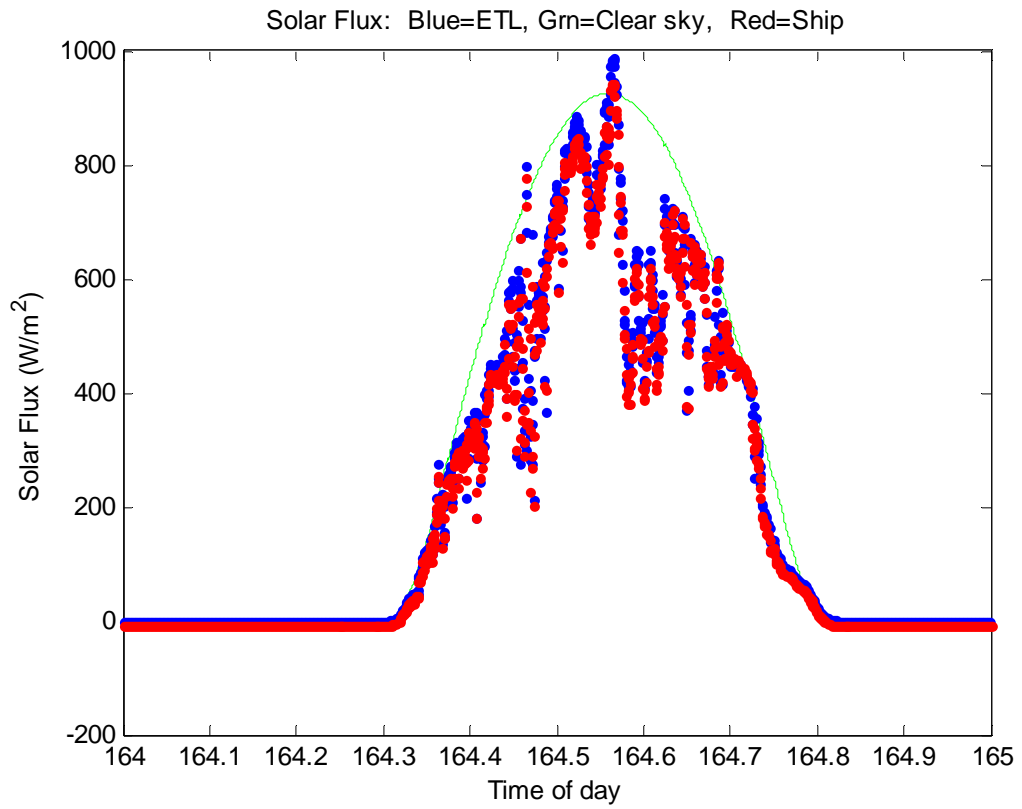


Figure 2. Time series of downward solar flux from ETL and ship Eppley sensors. The green line is a model of the expected clear sky value.

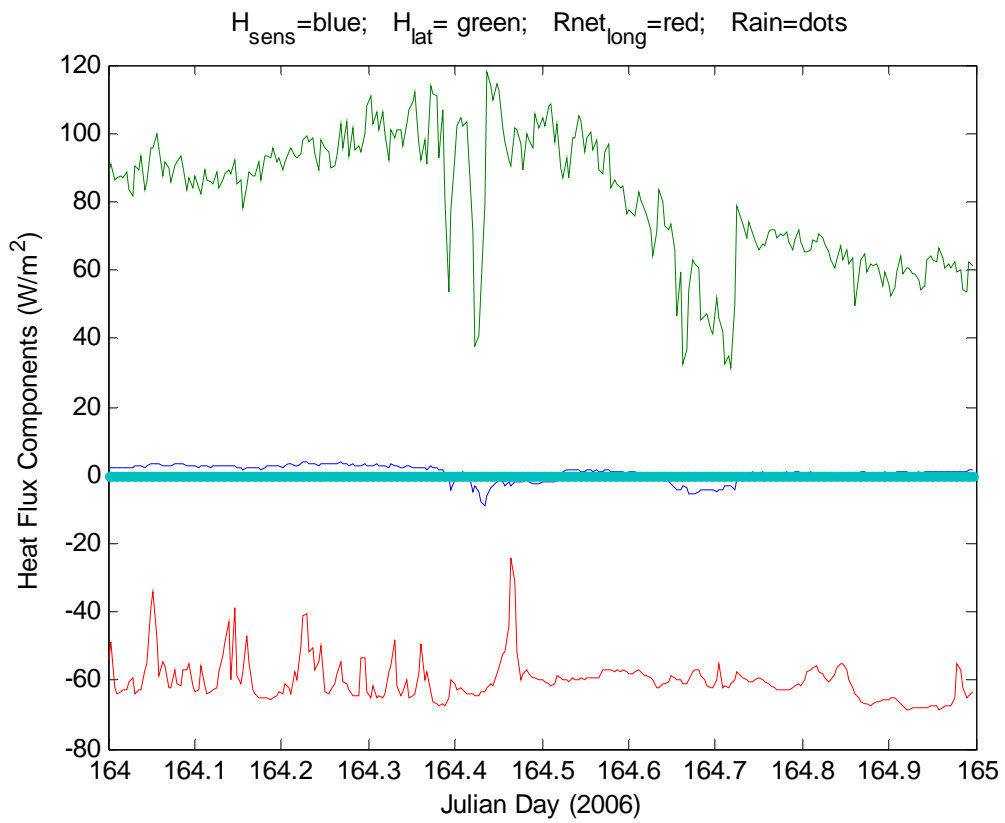


Figure 3. Time series of non-solar surface heat flux components: sensible (blue), latent (green), and net IR (red).

Heat Fluxes: Net= 60.6163; $H_{\text{lat}} = 81.0317$; $H_{\text{sens}} = 0.70595$; $R_{\text{short}} = 202.3547$; $R_{\text{long}} = -59.996$

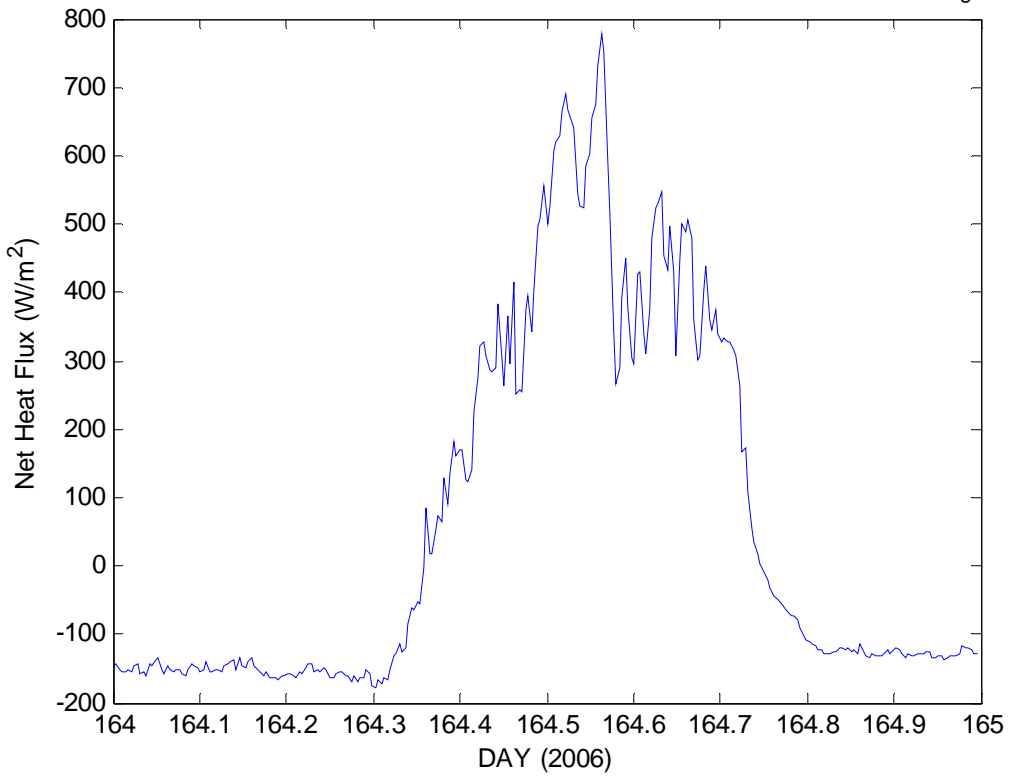


Figure 4. Time series of net heat flux to the ocean surface. The values at the top of the graph are the average for the day for each component of the flux.

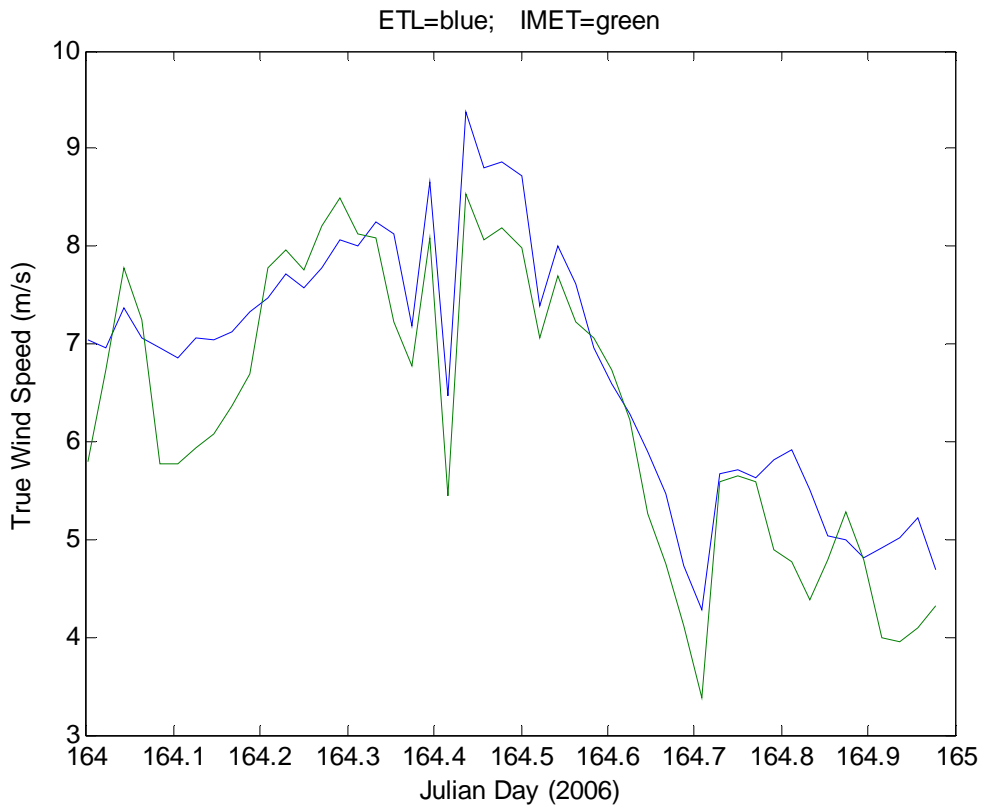


Figure 5. True wind speed from the ETL sonic anemometer (18 m) and the ship's propvane (15 m).

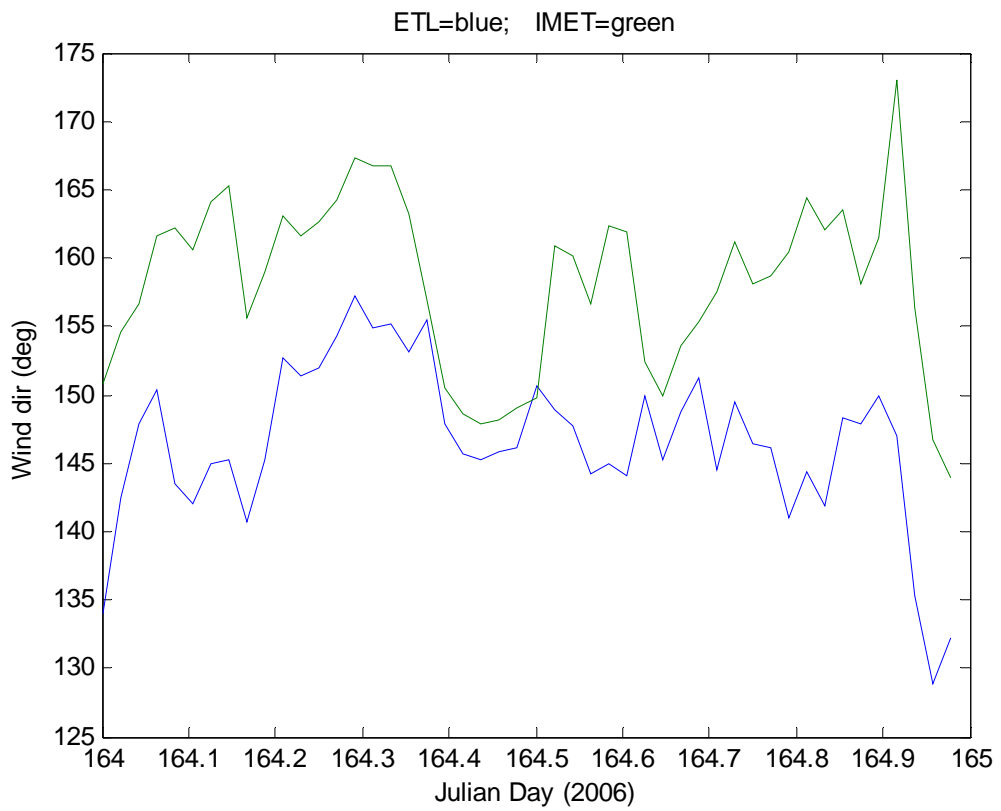


Figure 6. True wind direction from the ETL sonic anemometer (18 m) and the IMET propvane (15 m).

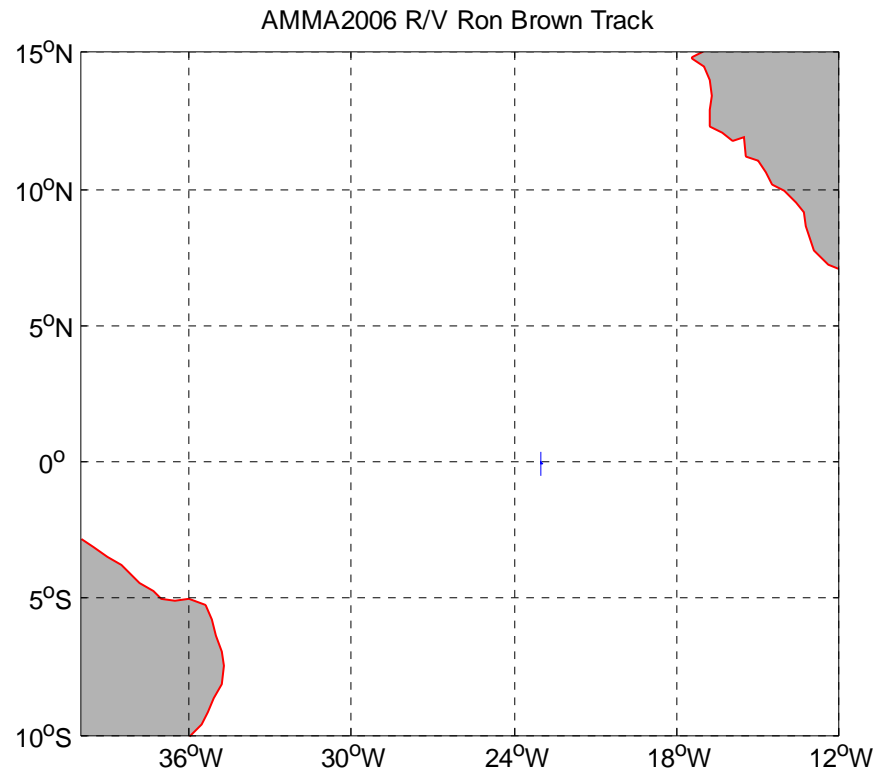


Figure 7. Cruise track for RBH on June 13 2006 (DOY 164).

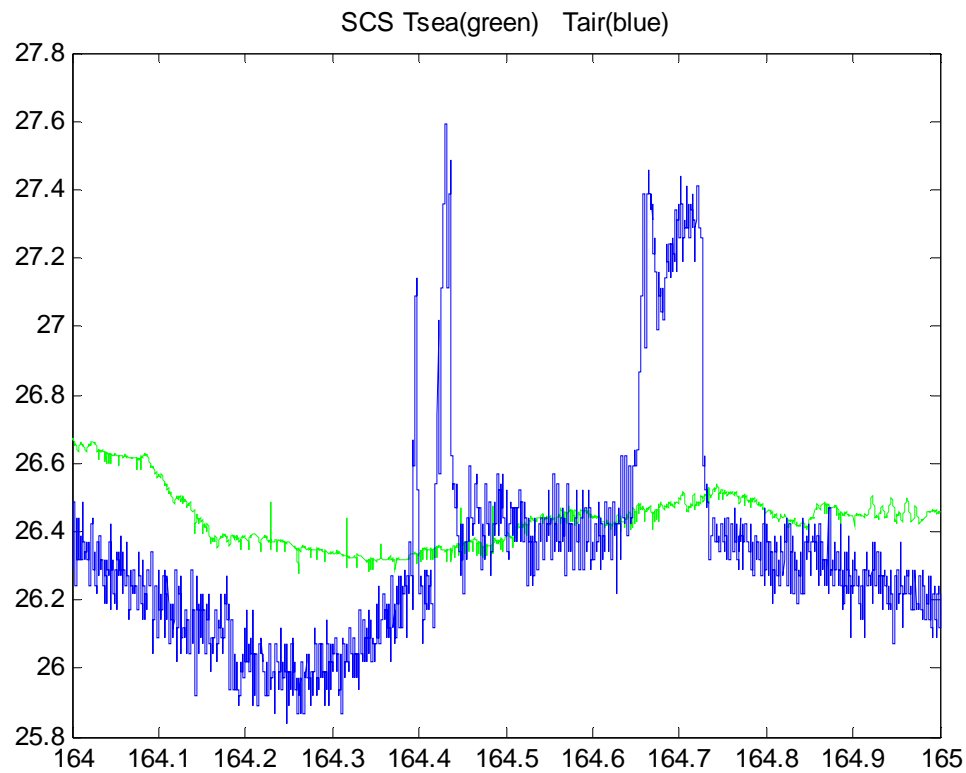


Figure 8. Time series of near-surface ocean temperature (green) and 15-m air temperature (blue).

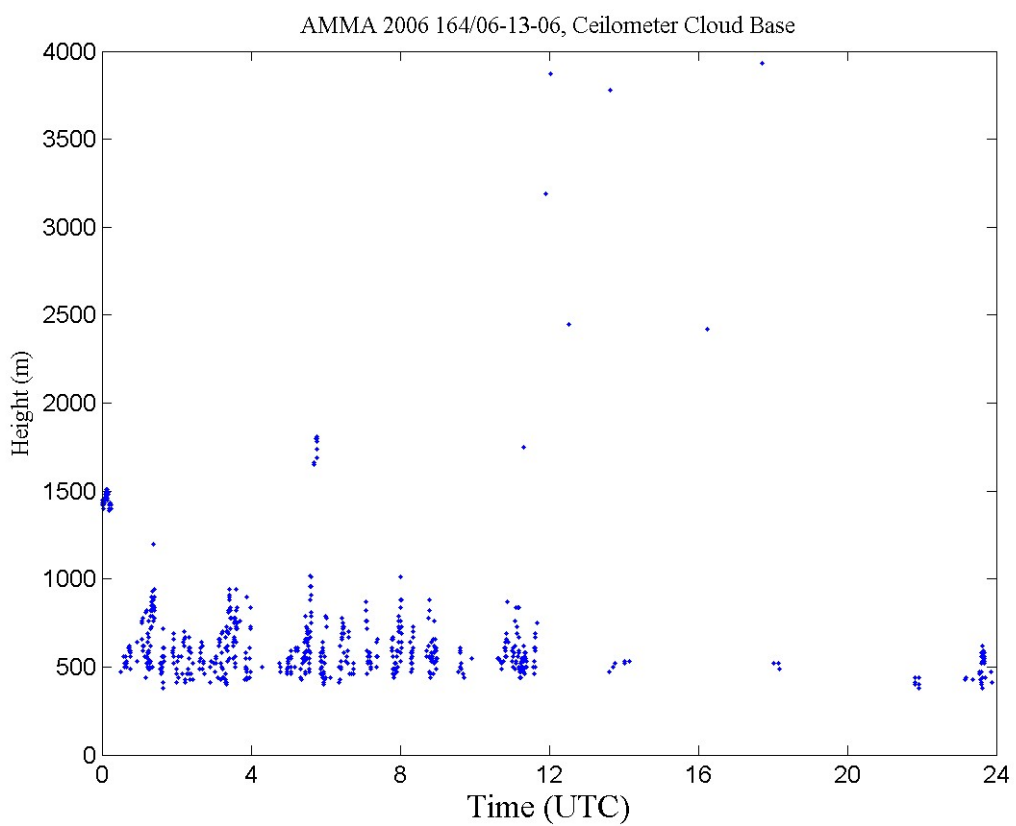


Figure 9. Cloud-base height information extracted from the ceilometer backscatter data for day 164 (June 13, 2006).

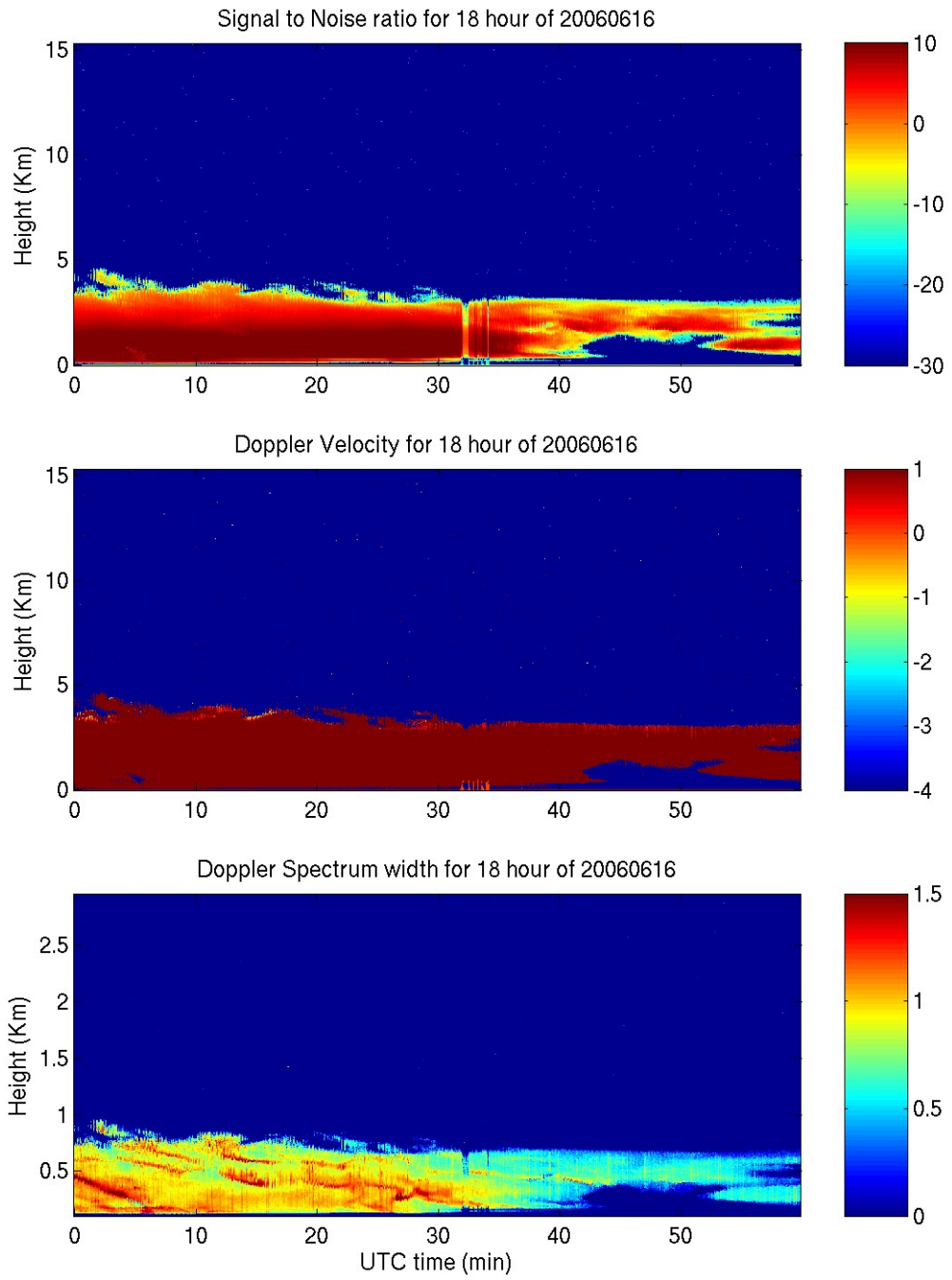


Figure 10. Time-height cross section data from 9.4 GHz cloud radar data for day 167 (June 16, 2006): upper panel, backscatter intensity; middle panel, mean Doppler vertical velocity; lower panel, Doppler width.

2. Cruise Summary Results

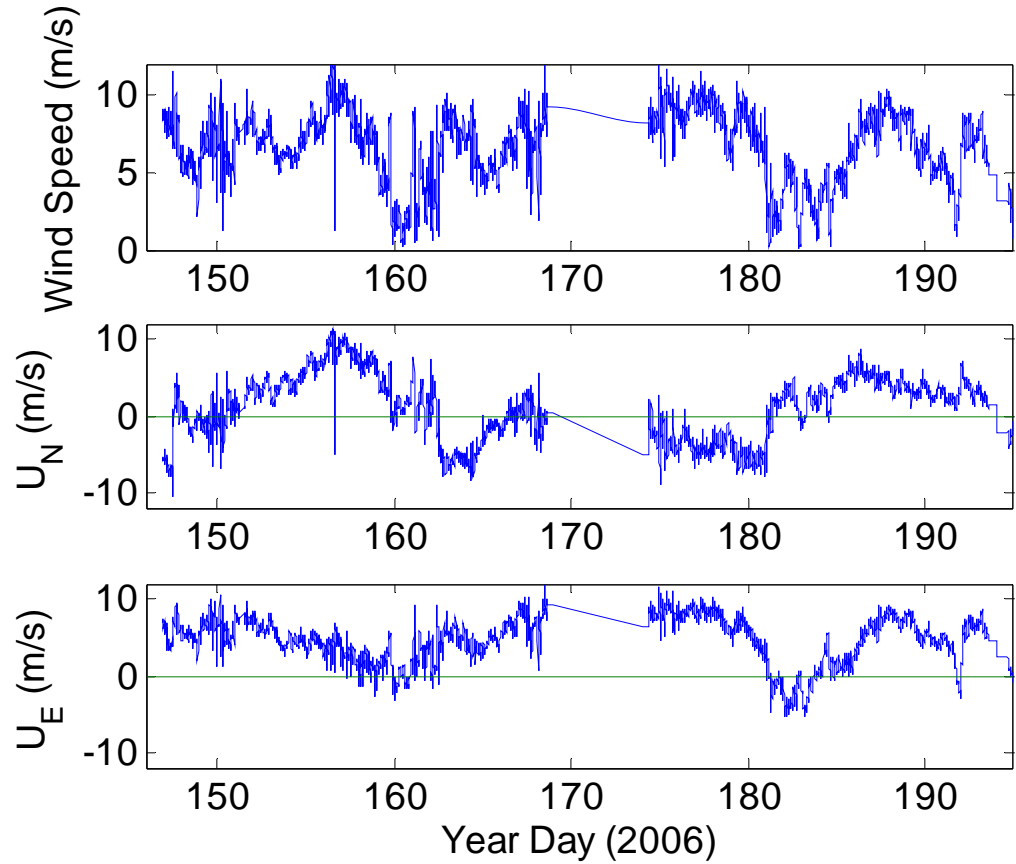


Figure 11. Time series of wind speed (upper panel), northerly component (middle panel), and easterly component (lower panel) for the 2006 RHB AMMA cruise.

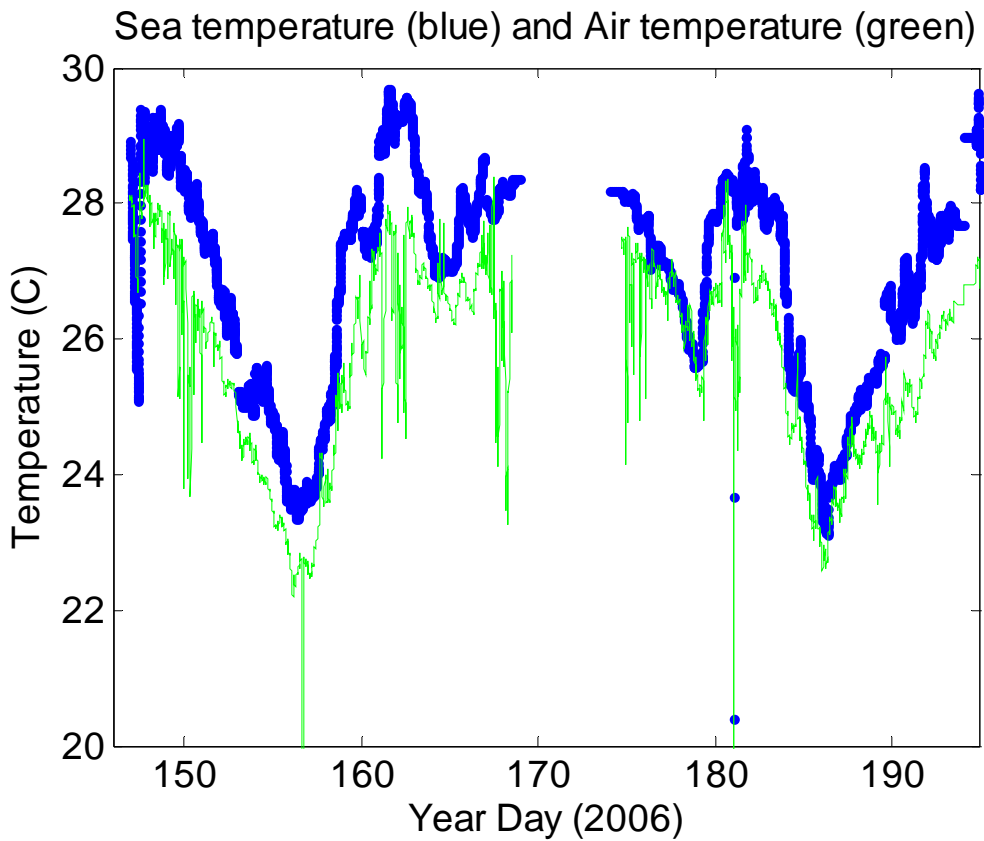


Figure 12. Time series of near-surface ocean temperature (blue) and 15-m air temperature (green) for the 2006 RHB AMMA cruise.

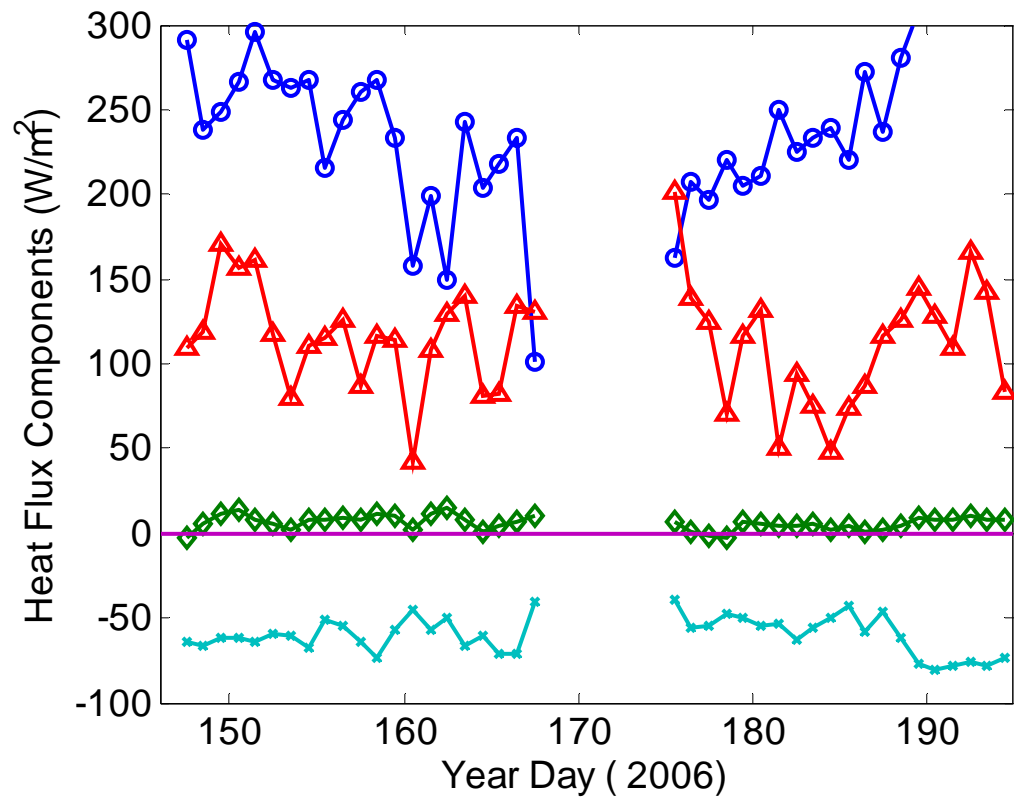


Figure 13. Time series of 24-hr average heat flux components: solar flux - circles; latent heat flux - triangles; sensible heat flux - diamonds; net IR flux x's.

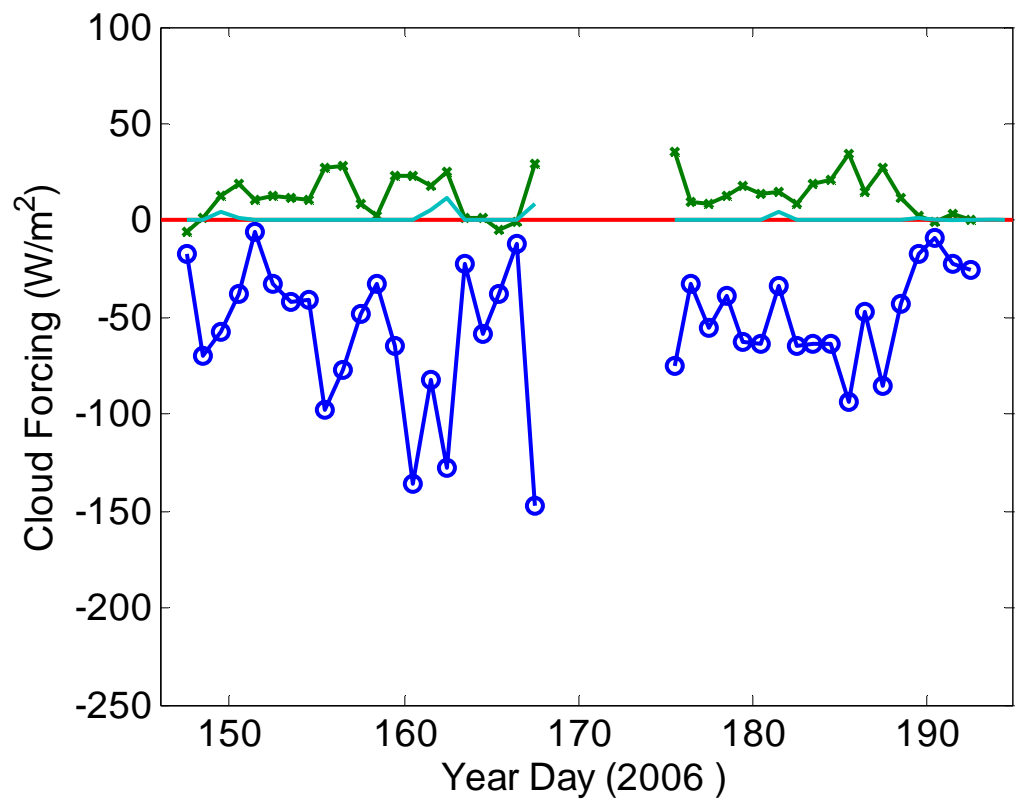


Figure 14. Time series of daily averaged radiative cloud forcing: IR CF (W/m^2) – green, Solar CF (W/m^2) – blue.

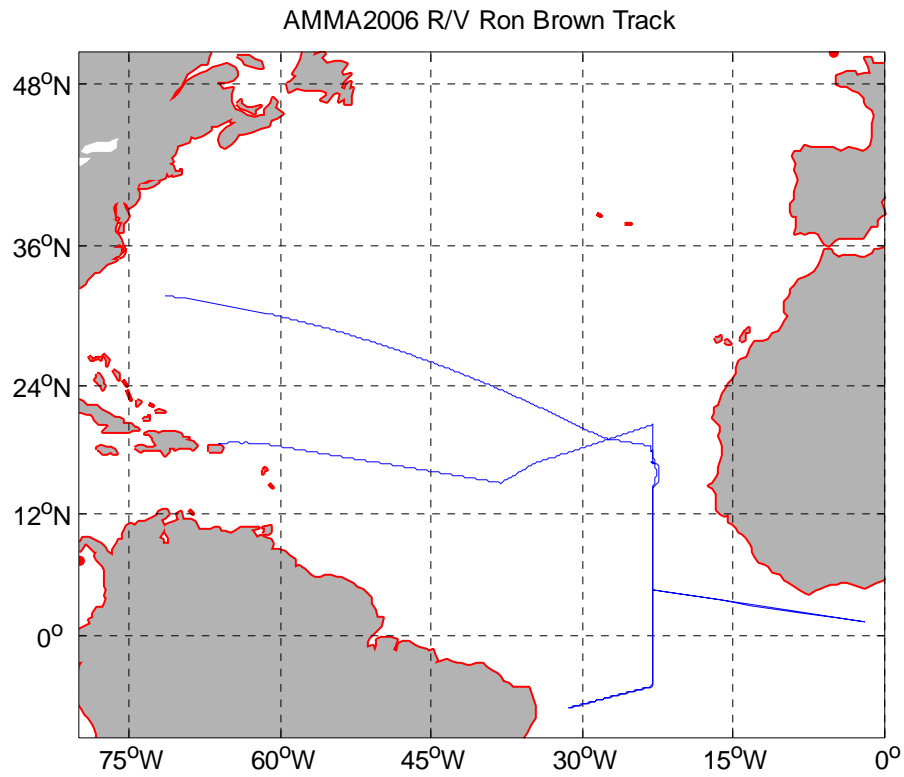


Figure 15. Cruise track for entire AMMA 2006 cruise.

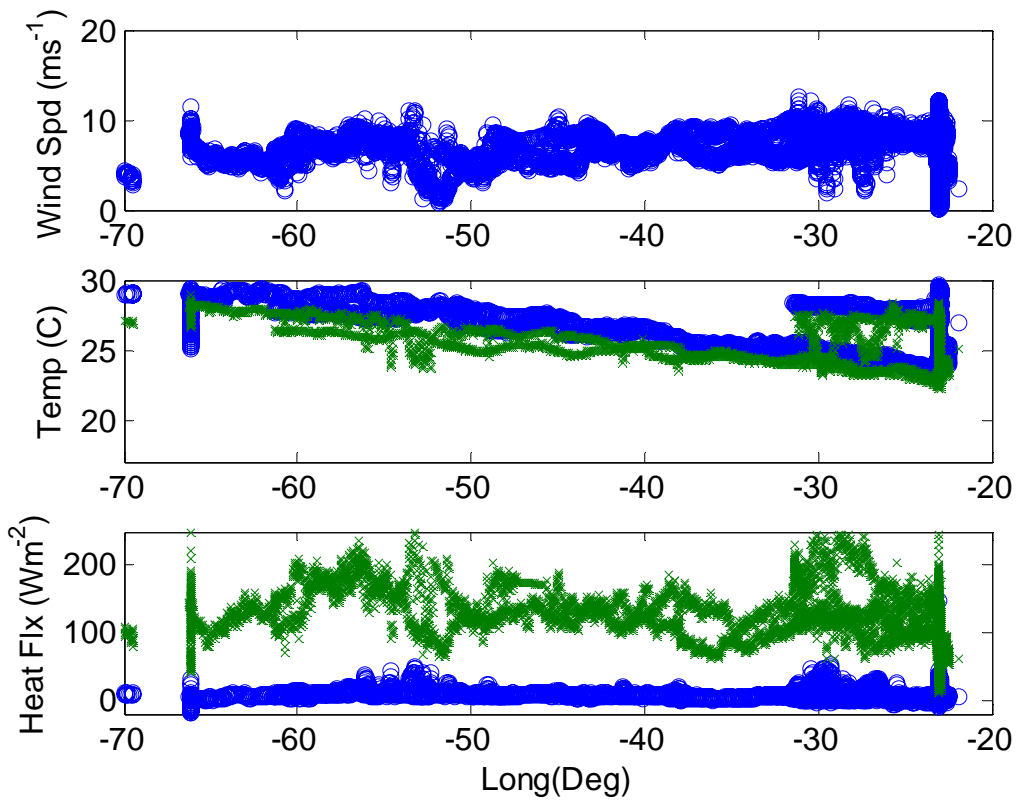


Figure 16. W-E plots of selected variables. Upper panel is wind speed; the middle panel is sea surface temperature (blue) and air temperature (green); the lower panel shows sensible (blue) and latent (green) heat fluxes.

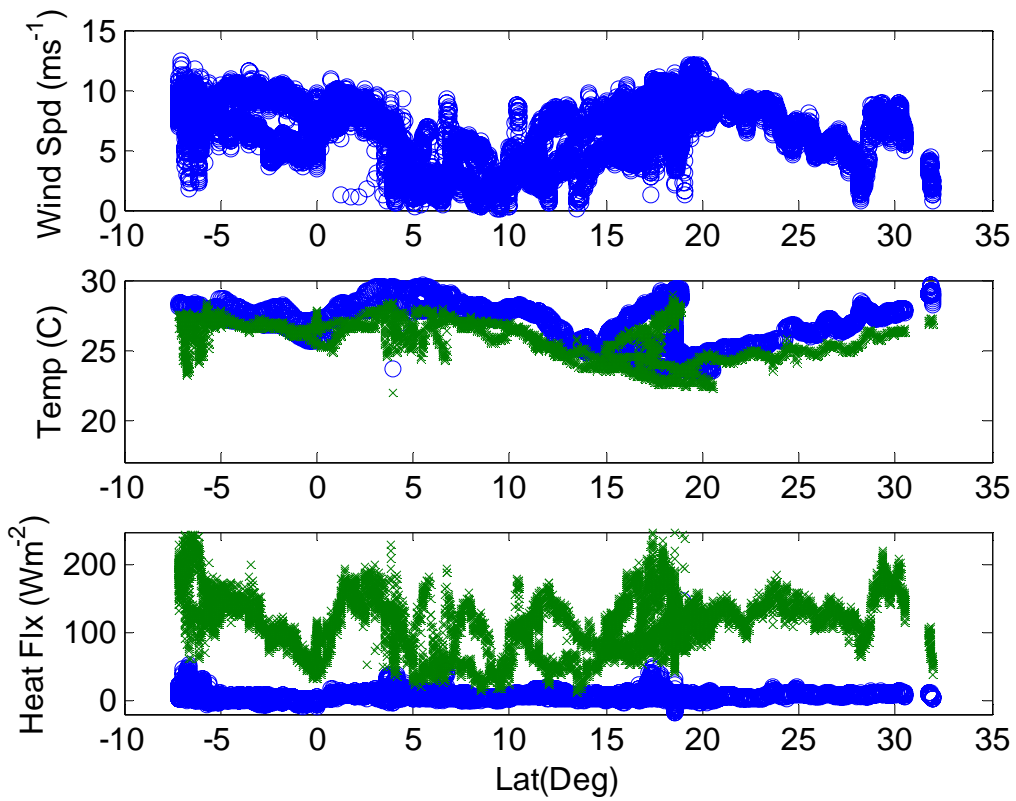


Figure 17. N-S plots of selected variables. Upper panel is wind speed; the middle panel is sea surface temperature (blue) and air temperature (green); the lower panel shows sensible (blue) and latent (green) heat fluxes.

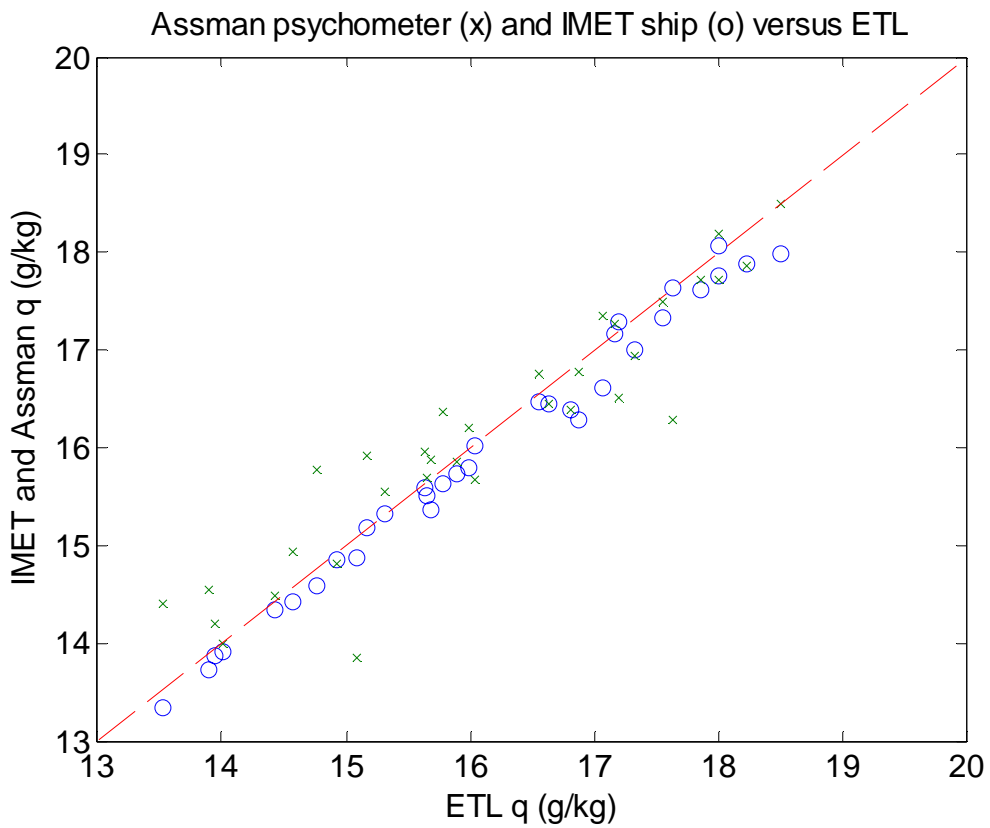


Figure 18. Comparison of simultaneous Assman psychrometer (x's) and ship (circles) readings for specific humidity. Psychrometer values corrected to 15 m (ETL and ship instrument height).

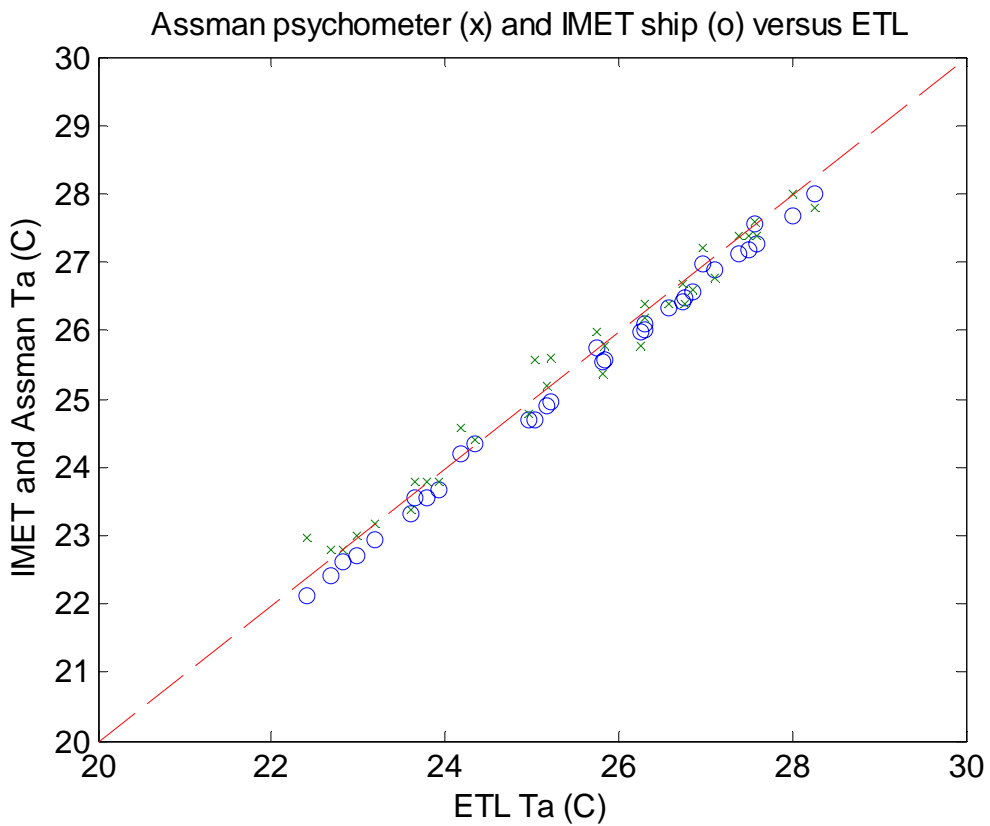


Figure 19 . Comparison of simultaneous Assman psychrometer (x's) and ship (circles) readings for air temperature. Psychrometer values corrected to 15 m (ETL and ship instrument height).

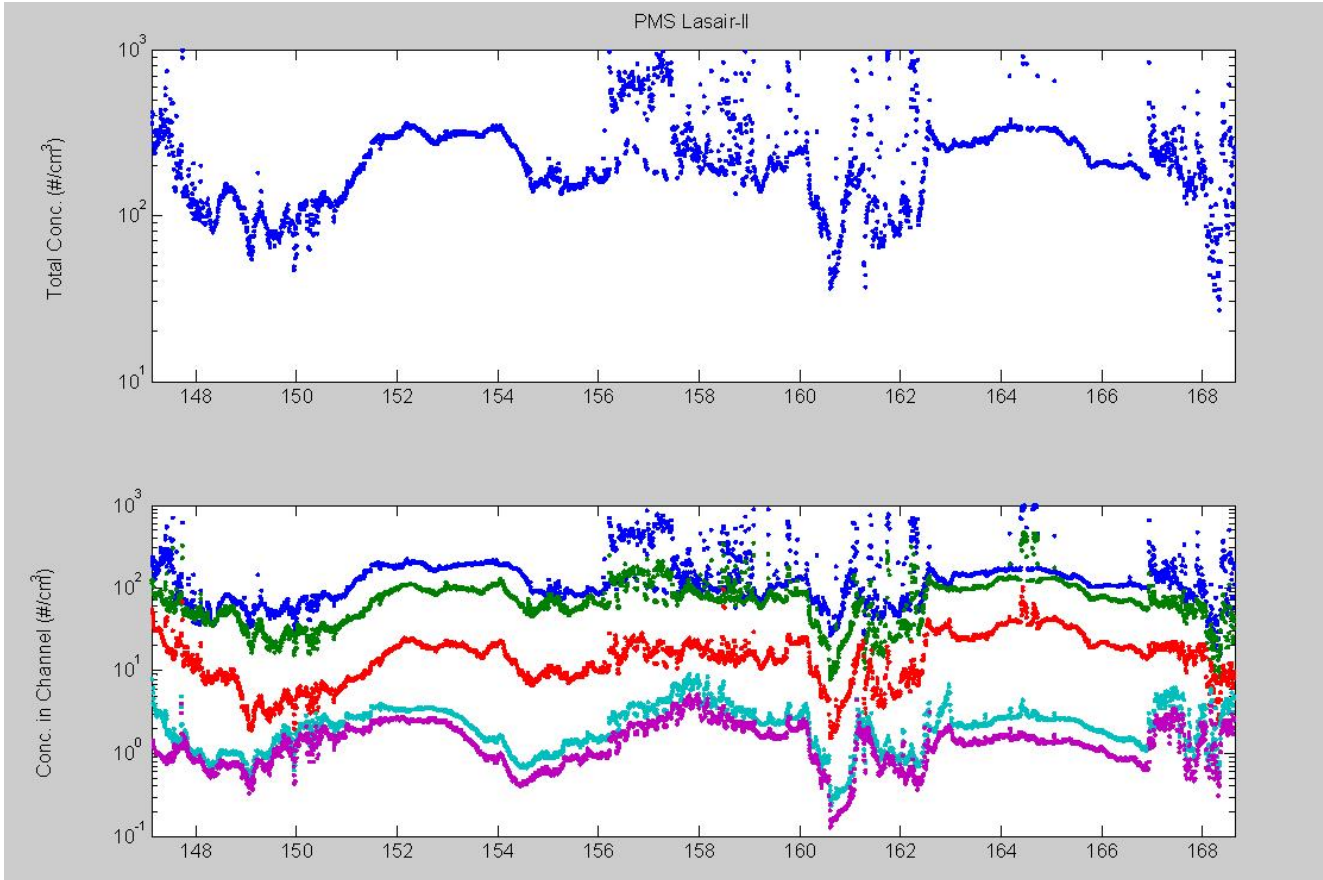


Figure 20. Aerosol concentrations from Lasair-II spectrometer for AMMA 2006 (leg1). Upper panel: total number concentration for aerosols larger than 0.1 micron diameter. Lower panel: aerosol concentrations for 0.1-0.2 (blue), 0.2-0.3 (green), 0.3-0.5 (red), 0.5-1.0 (cyan), and 1.0-5.0 (magenta). Spikes are caused by the ship's exhaust.